

Chapter 7

Putative Bioactive Conformers of Small Molecules: A Concerted Approach Using NMR Spectroscopy and Computational Chemistry

T. Mavromoustakos^{1,2}, S. Golic Grdadolnik^{3*}, M. Zervou²,
P. Zoumpoulakis², C. Potamitis^{1,2}, A. Politi^{1,2}, E. Mantzourani⁴,
J. A. Platts⁴, C. Koukoulitsa², P. Minakakis¹, G. Kokotos¹, T. Tselios⁵,
J. Matsoukas⁵, S. Durdagi^{2,7}, M. G. Papadopoulos², D. P. Papahatjis²,
Z. S. Spyranti⁶, G. A. Dalkas⁶ and G. A. Spyroulias⁷*

¹Chemistry Department, University of Athens, Zographou 15784, Athens, Greece

²National Hellenic Research Foundation, Institute of Organic and
Pharmaceutical Chemistry, 11635 Athens, Greece

³National Institute of Chemistry, Hajdrihova 19, 1001 Ljubljana, Slovenia

⁴Department of Chemistry, Cardiff University, P.O Box 9121, CF10, 3TB, Cardiff UK

⁵University of Patras, Chemistry Department, 26500 Rion, Patras, Greece

⁶University of Patras, Pharmacy Department, 26500 Rion, Patras, Greece

⁷Department of Biology, Chemistry and Pharmacy, Freie Universitat Berlin,
Takustr 3, 14195 Berlin, Germany

Abstract

The knowledge of a bioactive conformation of a known lead or potential lead compounds undoubtedly will offer a save of money and time consuming to pharmaceutical companies aiming towards the development of new drugs. This review article deals with the use of different approaches to explore conformers of biologically active molecules at various environments which may simulate the biological ones. The molecules under study are mostly synthetic organic, with low molecular weight or small peptides. Two of the major structural characteristics of these molecules are: (i)

amphiphilicity; and (ii) existence of flexible and rigid pharmacophoric segments. The rigid part of the molecule does not possess much of interest in terms of conformational analysis. However, the flexible segment constitutes a challenging field for conformational analysis exploring of putative bioactive conformations. NMR spectroscopy is a powerful tool to derive putative bioactive conformers of biologically active molecules. Application of 2D NOESY or ROESY spectroscopy could provide enough information for this purpose. Thus, quantitative analysis of the cross peaks reveals interatomic distances between the nuclei interacting through space. When a molecule contains bonds that restraint the molecular motion resulting in different distinct conformations detected by NMR spectroscopy, the use of 2D EXSY spectroscopy can differentiate between conformational exchange processes and spatial interactions. Molecular Modeling (Computational Chemistry) is a supplementary tool for providing the visual means to medicinal chemists, who are interested in the design and synthesis of novel bioactive molecules. Thus, energy minimization algorithms, conformational analysis tools like grid scan, Monte Carlo and molecular dynamics simulations in combination with the experimentally derived distance restraints will determine the putative bioactive conformers. Conformational analysis in a simulated environment is not always sufficient. The derived low energy conformers within a range of energy should be docked in the active site of the receptor. In many cases, drug molecules containing flexible segments can easily adopt conformations with higher energies in the biological matrices or at the active site of the receptor. The increase of energy is then compensated by the many different favorable interactions. In some cases, Quantum Mechanics calculations are useful and can be more informative in terms of conformational analysis. For example, chemical shift simulation of NMR spectra may screen low energy conformers derived from the coupling of conformational analysis techniques and NMR spectroscopy. Moreover, 3D QSAR studies provide valuable structural information concerning the optimum bioactive conformation.

Introduction

It is well known that only one out of the thousand of those compounds synthesized will successfully pass the time consuming and expensive processes of preclinical and clinical phases. The decisive and most expensive step in the development of a new medicine is the synthesis of the appropriate bioactive compound which will be formulated and commercialized. Pharmaceutical companies would greatly reduce the drug cost if the lead compound to start the synthetic strategic plan was known not only structurally but also conformationally. It is not therefore surprising that pharmaceutical companies are strongly interested to know the bioactive conformations of existing and potentially future drug molecules. Such information will aid in the design and synthesis of novel molecules possessing optimized biological activity.

This brief discussion brings up the following question. Are the medicinal chemists able to help the pharmaceutical companies to reduce their expenses by providing lead compounds with known conformational properties? Thanks to tremendous advances in biotechnology and molecular modeling which today offer more than ever in the past opportunities in this demand of pharmaceutical companies. Such scientific advancements which provide this facility to pharmaceutical companies are briefly summarized below:

- 1) *Molecular Biology-Biotechnology*; isolation, identification and structure determination of biomolecules related to human diseases opened new avenues to drug design. This kind of molecules also involves protein receptors, which play a significant role in inducing biological activity through ligand binding process.
- 2) *Experimental techniques*; High field NMR (Nuclear Magnetic Resonance) spectroscopy, synchrotron radiation X-ray crystallography, novel techniques on IR (infrared) and Raman spectroscopies provide valuable information in terms of the low energy conformation of a molecule in a crystal state or in an environment that simulates the biological one.
- 3) *Novel in silico approaches*; together with improved computational power, software for molecular modeling techniques using Molecular Mechanics or Quantum Mechanics, provide information on the conformational properties of drug molecules, physicochemical properties, ligand-receptor binding information, interactions with lipid bilayers, pharmacokinetic and pharmacodynamic properties. Use of QSAR (quantitative structure analysis relationships) offer new means for design and synthesis of novel analogs and provide new approaches in the design of conformationally defined molecules with predicted activity. Furthermore, when receptors are difficult to be isolated (such as transmembrane receptors) template models are developed based on theoretical calculations.

Rational Drug Design is based on the above mentioned scientific advances and combines theoretical calculations and experimental techniques. In this review article, synthetic organic molecules and small peptides of biological importance are conformationally explored at various environments.

Two are the major structural characteristics of these molecules: (i) amphiphilicity, and (ii) flexible and rigid pharmacophoric segments. The rigid part of the molecule does not possess much of interest in terms of conformational analysis while the flexible segment constitutes a challenging field for conformational exploration of putative bioactive conformers.

NMR spectroscopy has proved to be an experimental powerful tool for the study of putative bioactive conformers of biologically important molecules [1, 2]. Since we will restrain our review using low molecular weight molecules, quantitative 2D NOESY or ROESY techniques can provide sufficient information for conformational analysis. Quantitative analysis of the experimental data provides interatomic distances of nuclei being in a spatial proximity less than 5Å. This data refine the initial low energy conformers produced by simple energy minimization procedures. When NMR detects distinct conformations of a molecule in solution, 2D EXSY is mostly used in Dynamic NMR Spectroscopy providing valuable information concerning the equilibrium between conformations.

As previously noted, NMR Spectroscopy is combined with Molecular modeling in order to reveal low energy bioactive conformers. The conformational space is explored using systematic and stochastic algorithms based on Molecular and Quantum Mechanics and several force fields. In addition, simulation of IR and NMR spectra using QM calculations provide complementary data for the determination of putative bioactive conformers.

Moreover, conformers produced from *in silico* docking studies are of great importance as they are based on the interactions between the ligand and the active site of the receptor. Several

docking methodologies can be applied including or not the conformational flexibility of the ligand and the receptor.

3D QSAR studies characterized by ligand-based alignment are used for the development of predictive models necessary for the improvement of the molecular structure for optimum activity. The Figure 1 describes briefly the usual process used in the conformational analysis of biologically important molecules.

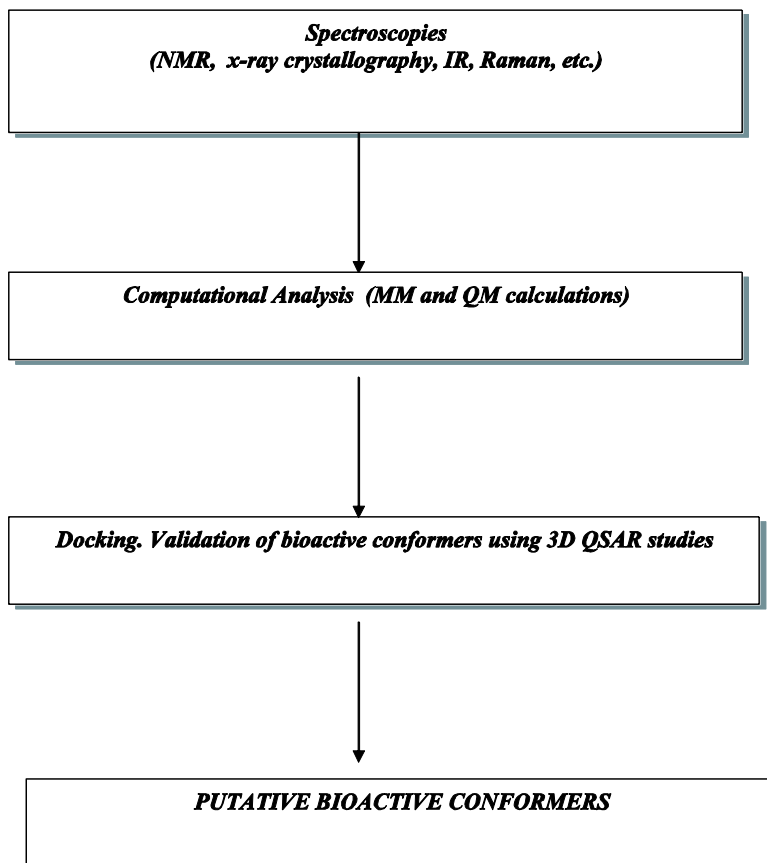


Figure 1. Procedure followed to derive putative bioactive conformers.

Conformational Analysis of AT₁ Antagonists

RAS constitutes the major system that regulates blood pressure. Therefore, it has been targeted in the drug design for developing novel synthetic antihypertensive drugs. The first rationale behind the synthesis of novel angiotensin analogs was to block the formation of vasoconstrictive hormone angiotensin II. Renin and angiotensin converting enzymes are responsible for the transformation of angionsinogen to angiotensin I and subsequently to angiotensin II in the body. The blocking of angiotensin converting enzyme was crown with success and the market experienced captopril and its congeners as beneficial molecules in blood regulation. However, their side effects of dry mouth and angioedema preclude them for being

the ideal drugs for hypertension. Renin inhibitors block the formation of Ang I and subsequently Ang II. The first synthetic molecules were peptide or peptide like molecules and since they were easily metabolized did not possess the desired activity [3]. Only recently, the synthetic molecule aliskiren entered the market (Rasilez, Novartis) with success [4]. The second class of synthetic molecules aimed in the blocking of angiotensin II at AT₁ receptor [5-10]. The first peptide analogs synthesized for this aim although not successful, they aided in providing molecular models for rationale design [11]. Losartan was the first successful peptidomimetic analog to be marketed and its synthesis was based on the C-terminal conformational segment of Angiotensin II model proposed by *Fermadjian et al.* [12]. Angiotensin receptor blockers (ARBs) have been developed to produce a more complete blockade of the action of angiotensin II as compared to other drug classes, as well as an improved side effect profile [13]. Although, several drugs have been launched for the regulation of high blood pressure through the RAS cascade, intense research activity is still necessary to explore the structure requirements that direct to more effective antihypertensive drugs deprived of side effects. Due to the great need of more effective antihypertensive drugs, our laboratory has initialized a long term research activity for the Rational Design of novel AT₁ antagonists mainly based on the conformational properties of marketed and synthetic molecules.

A representative conformational part of the study referred to prototype AT₁ antagonist losartan is shown below. The molecule was first structurally analyzed using a series of 1D and 2D NMR experiments. A 2D ¹H-¹H DQF COSY is shown in Figure 2. The conformational analysis was based on data from 2D ¹H-¹H ROESY experiments and was performed in different environments (a) DMSO, (b) D₂O, and (c) micelles solution. Figure 3 depicts a representative 2D ¹H-¹H ROESY in DMSO while Figure 4 shows the ¹H NMR profile of losartan in the three different environments. Quantitative analysis of 2D ROESY spectra and Molecular Modeling studies revealed low energy conformers for the three environments. A representative putative bioactive conformation of losartan is shown in Figure 5 [14, 15].

Valsartan (Diovan) is the second orally active non-peptide angiotensin II specific to AT₁ receptor antagonist to reach the market in Europe and the USA for the treatment of hypertension. Several dose-findings and comparative studies have demonstrated that valsartan is an effective and well tolerated antihypertensive drug in patients with mild to moderate hypertension and to be effective in severe hypertension. Its effectiveness is at least equivalent to ACE inhibitors, diuretics, β-blockers and calcium antagonists and it has the advantage that does not cause cough and lower limb edema as ACE inhibitors [16-24].

Valsartan differs structurally from losartan in that its heterocycle has been replaced by an alkylated aminoacid. Like Losartan, its rational design is based on the mimicry of the C-terminal segment of Ang II.

Two distinct conformations of valsartan were observed from integral inspection of the ¹H NMR spectrum (Figure 6). These are attributed to the hindered rotation around its amide bond.

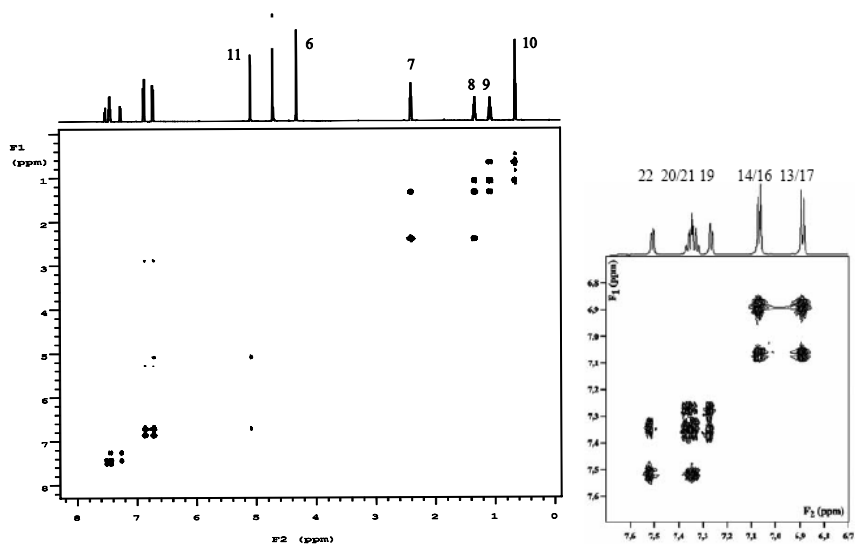


Figure 2. 2D COSY-DQF of losartan at 25 °C in D₂O. The assignment is shown on the top of the peaks.

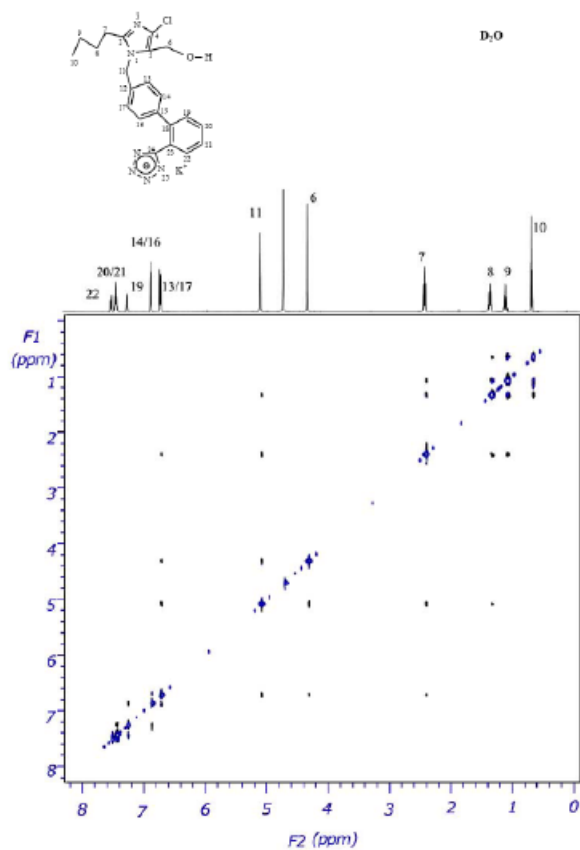


Figure 3. 2D ROESY of losartan at 25 °C in D₂O.

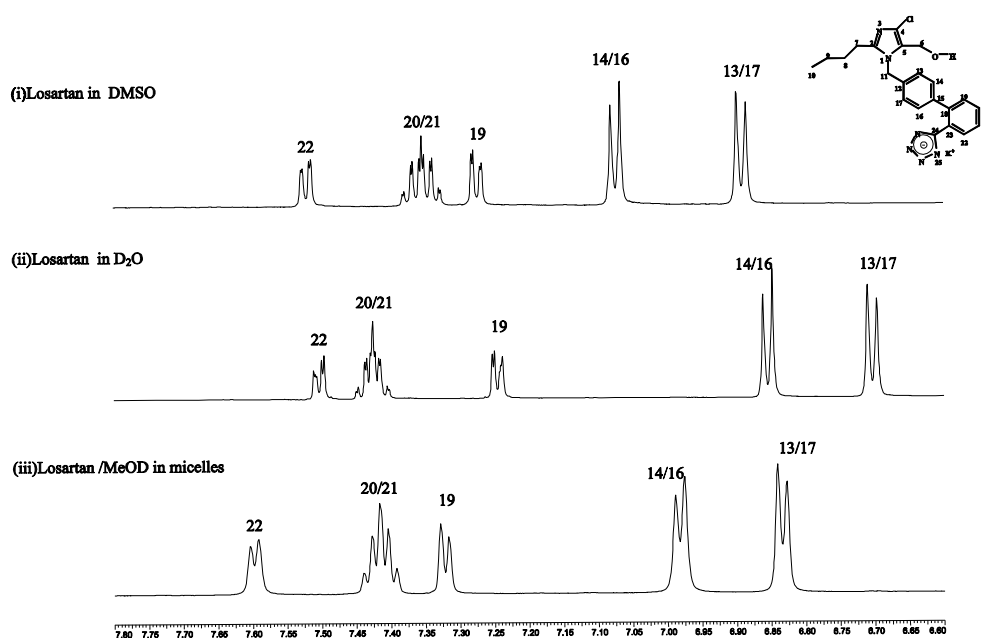


Figure 4. ^1H NMR representative spectra of losartan in DMSO, D_2O , and micelle solution. Additional peaks in the methyl region of losartan in micelles are due to the detergent alkyl chain resonances.

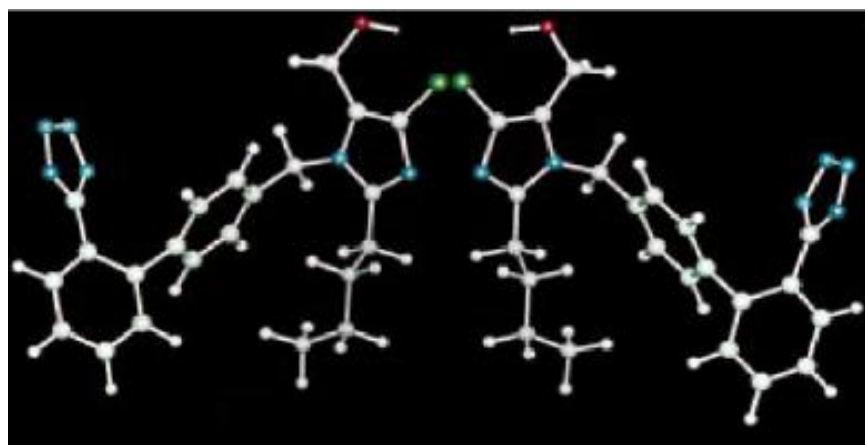


Figure 5. Proposed enantiomeric conformers of losartan.

For the complete assignment of proton resonances of valsartan are used the through bonds interactions depicted in 2D DQF-COSY spectrum and the observed through-space proton correlations in the 2D ROESY spectrum. Work is under progress to estimate the barriers for the two distinct conformations and their interactions at the receptor site.

Based on superimposition studies of losartan with the model proposed for sarmesin, a new avenue was explored in an attempt to design and synthesize novel AT1 antagonists. Thus, few years ago we have briefly reported MMK1 synthesis, a simple molecule which possesses

pyrrolidinone instead of biphenyltetrazole template. Its stereoelectronic properties were also analyzed and compared with those of losartan [25].

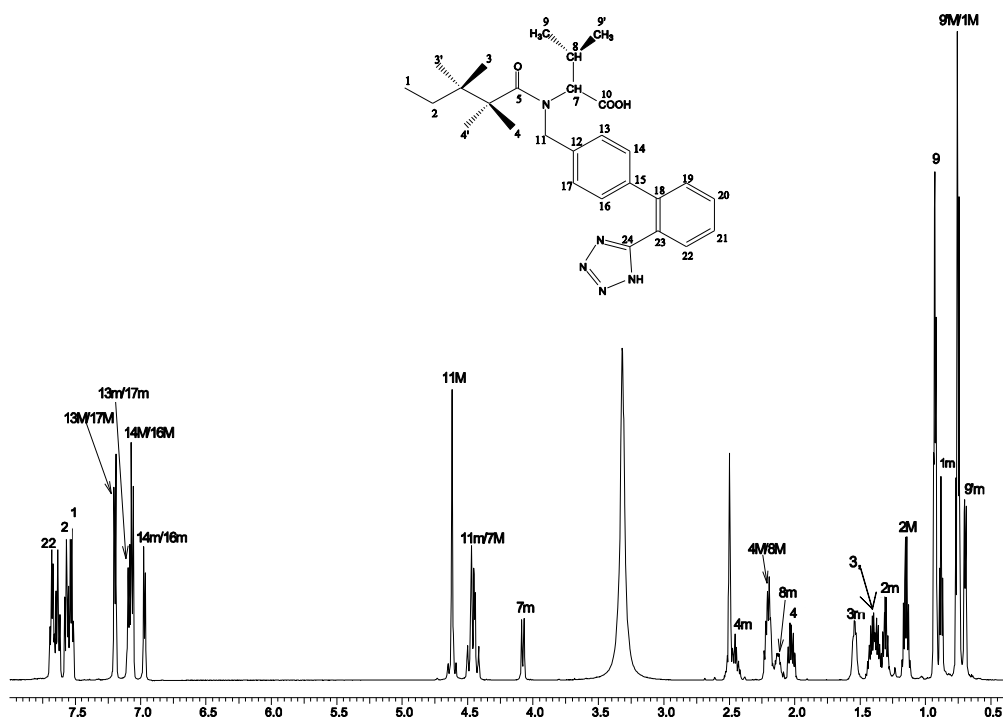


Figure 6. ^1H NMR spectrum of valsartan.

MMK1 was designed to mimic conformational characteristics of His6-Pro7- Phe8 and constitutes the first lead compound. Two other derivative compounds were also synthesized namely MMK2 and MMK3. The structures of losartan, MMK1, MMK2, and MMK3 are shown in Figure 7 and their synthesis in Figure 8 [26, 27]. In addition, comparative *in vitro* binding studies with AT_1 and AT_2 receptors are performed, as well as *in vivo* experiments with adult normotensive male New Zealand White rabbits. All molecules were found to be less active than prototype losartan. Moreover, theoretical (docking) studies were applied to investigate possible interactions between the molecules with binding amino acids. Such studies may aid to provide a plausible explanation for the *in vivo* and *in vitro* results strengthening the rational design of novel analogs with improved binding affinities. As it can be seen from the docking of MMK1 at AT_1 antagonist the molecule possesses only hydrophobic interactions. Acidic moieties (i.e. carboxylate group or an isosteric tetrazole) are necessary in order to form electrostatic interactions or hydrogen bonds between MMK derivatives and the AT_1 receptor pocket (Figure 9). Such molecules are underway to be synthesized.

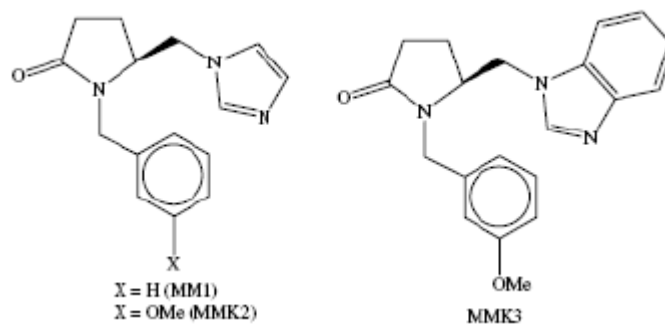


Figure 7. Chemical structures of MMK1 (MM1), MMK2, and MMK3.

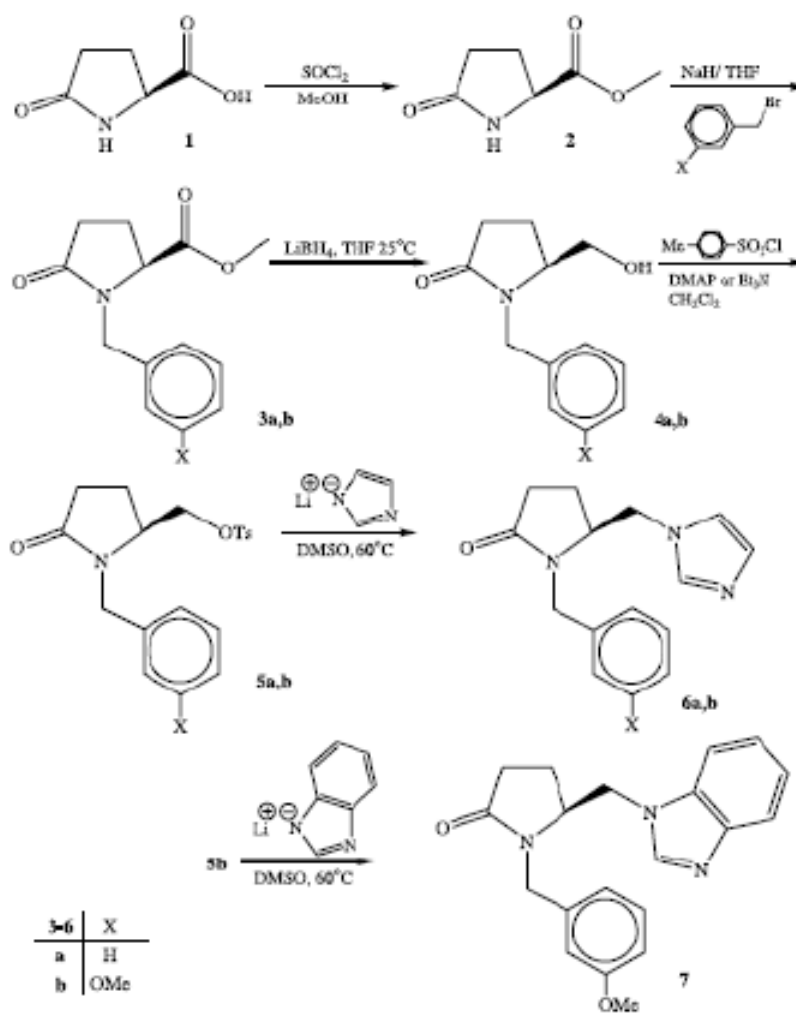


Figure 8. Synthesis of (5S)-1-benzyl-(1H-imidazol-1-yl-methyl)-2-pyrrolidinone (MM1), (5S)-1-(3-methoxybenzyl)-5-(1H-imidazol-1-ylmethyl)-2-pyrrolidinone (MMK2), and (5S)-1-(3-methoxybenzyl)-5-(1H-benzimidazol-1-ylmethyl)-2-pyrrolidinone (MMK3).

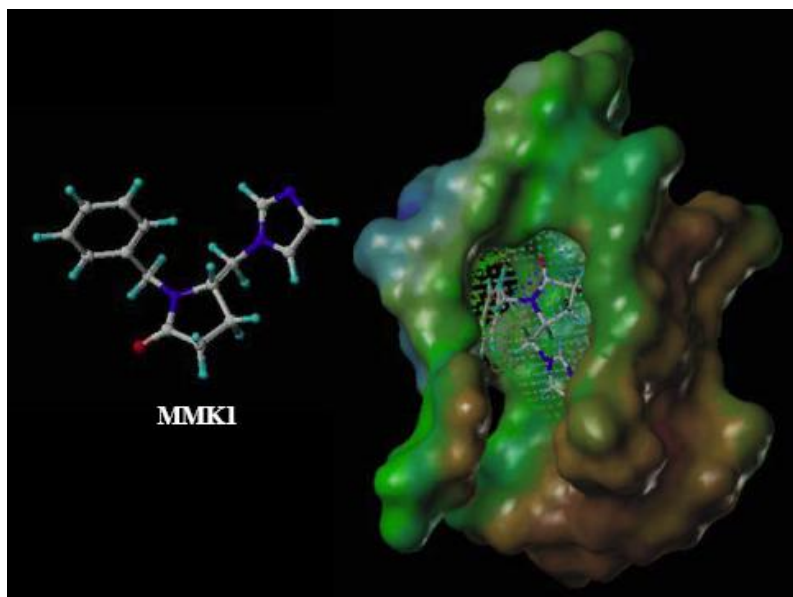


Figure 9. The incorporation of MMK1 in the putative pocket of AT1 receptor as it is revealed using theoretical and experimental data.

Conformational Analysis of Cannabinoids

Cannabis sativa L. is one of the oldest known medicinal plants and has been extensively used with respect to its psychotropic and pharmacological effects. Δ^9 -tetrahydrocannabinol (Δ^9 -THC), (Figure 10) is the primary psychoactive constituent of cannabis and it was identified by Gaoni and Mechoulam in 1964 [28].

The pharmacological activity of cannabinoid (CB) ligands is mediated by two CB receptors: CB1 [29] and CB2 [30]. Both CB1 and CB2 receptors belong to the Class A, membrane-bound rhodopsin-like family of G-protein coupled receptors (GPCR), possessing seven characteristic transmembrane domains [31]. The CB1 receptor is abundant especially in the central nervous system (CNS) and peripheral tissues [32]. The CB2 receptor, on the other hand, is exclusively present in the tonsils and cells of immune system [33]. Pharmacological studies have shown that CBs possess many potential therapeutic applications including; against cancer, AIDS, stroke, pain, obesity, cachexia and neuronal disorders such as multiple sclerosis, Huntington's chorea and Parkinson's disease, as well as reduction of blood ocular pressure in glaucomic patients [34-42].

The structure-activity relationship (SAR) studies have been reviewed comprehensively by Thakur [34], by Khanolkar [36], by Razdan [43], and by Makriyannis and Rapaka [44]. Earlier literature reports showed that the lipophilic alkyl side chain plays a crucial role in determining cannabimimetic activity and selectivity towards CB receptors, as well as pharmacological potency. The alkyl side chain fits into a hydrophobic pocket such that the chain is oriented nearly perpendicular to the aromatic ring A. Both synthetic and classical CB ligands contain a rigid segment and a flexible alkyl side chain. Structural variations of the *n*-pentyl group of natural CBs and endocannabinoids can lead to a wide range in affinity and

selectivity for the CB receptors CB1 and CB2, as well as their pharmacological potencies. Classical CB analogues with alkyl side chains of less than five carbon atoms have limited affinity for the CB1 receptor. Extension of the five carbon atom chain by adding one or two carbon atoms favors binding, while further extension is detrimental [34, 36]. Manipulation of the side chain can produce high-affinity analogues with antagonist, partial agonist, or full agonist effects [31]. Therefore, information based on the conformational properties of alkyl side chain will be useful for the design of new CB analogues with enhanced activity and other tailored properties.

In order to improve the medicinal properties and eliminate or reduce untoward effects, medicinal chemists are designing, synthesizing and testing additional CB1 and CB2 ligands. One of the main effort of our laboratory is to explore the pharmacophoric requirements of the alkyl side chain within the classical Δ^8 -tetrahydrocannabinol (Δ^8 -THC), and cannabidiol (CBD) templates (Figure 10). Δ^8 -THC has a very similar pharmacologic profile as Δ^9 -THC, however it is chemically more stable. Hitherto, 1',1' dithiolane Δ^8 -THC analogue (-)-2-(6a, 7, 10, 10a-tetrahydro-6, 6, 9-trimethyl-1-hydroxy-6H-dibenzo [b, d]pyranyl)-2-hexyl-1, 3-dithiolane (**12** in Table 1) is considered one of the most potent synthetic CB ligands. Therefore, in a previous study [45] we have explored its conformational properties using a combination of NMR spectroscopy and Molecular Modeling. Due to its high flexibility of alkyl chain we sought the aid of 3D QSAR and docking studies in order to reveal putative bioactive conformation of this molecule. We will skip its conformational analysis since it is straightforward and identical to that applied for AT₁ antagonists. We will emphasize how 3D QSAR and docking experiments will aid in the revealing of potential bioactive conformation.

To our knowledge until now, no direct observation of a CB ligand bound to a CB receptor using X-ray crystallography has been reported [46]. Therefore, active sites of these receptors have been postulated from many approaches, such as receptor binding analyses of a variety of CB derivatives using wild type and mutated receptor systems, molecular modeling analysis and three-dimensional quantitative structure-activity relationship (3D QSAR) studies [46-52]. Results of studies on 3D QSAR models of novel CBs using comparative molecular similarity indices analysis (CoMSIA), developed by G. Klebe *et al.*, [53] have been represented.

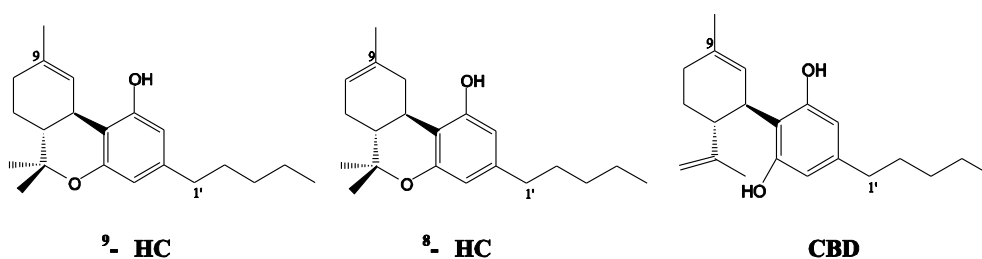
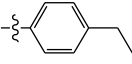
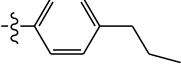
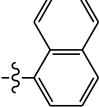
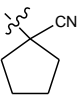
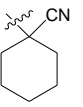
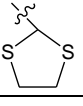
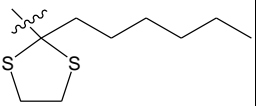
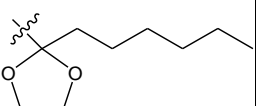
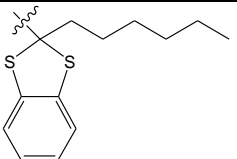
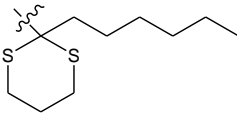
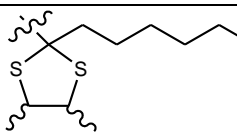
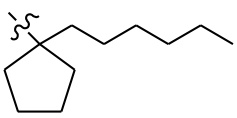
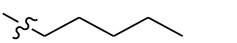
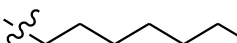
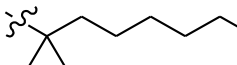
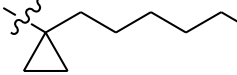
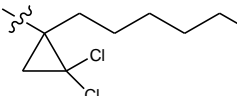
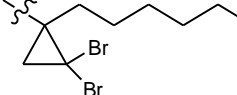
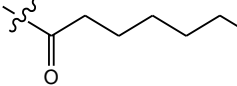
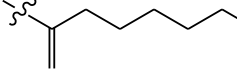


Figure 10. Chemical structures of Δ^9 -THC, Δ^8 -THC, and CBD.

Table 1 lists all structures used in the training set and their K_i values at the CB1 and CB2 receptors [54-58].

Table 1. Molecular structures and binding affinity K_i values of CB analogues used as the training set to construct CoMFA and CoMSIA models [54-58]

Compound No.	R	K_i for CB1 receptor (nM)	Compound No.	K_i for CB1 receptor (nM)
1		95.49	2	638.1
3		119.0		
4		57.77		
5		11.73	6	753.5
7		27.90	8	255.0
9		8.26	10	319.0
11		168.0		
12		0.32	13	136.0
14		0.52		

Compound No.	R	K_i for CB1 receptor (nM)	Compound No.	K_i for CB1 receptor (nM)
15		56.90		
16		1.80		
17		32.30		
18		0.45		
19		47.60	20	1265.0
21		22.00		
22		0.83		
23		0.44	24	58.68
25		1.27	26	666.4
27		0.71	28	189.0
29		21.70		
30		2.17		

Among the synthesized analogues, 12 was selected as a template, because: (i) the lowest energy conformer of 12 has been obtained and reported using a combination of NMR spectroscopy and molecular modeling techniques, previously [45] (ii) it has the highest binding affinity to the CB1 receptor ($K_i = 0.32$ nM) and second highest binding affinity to the CB2 receptor ($K_i = 0.52$ nM) in the training set.

Determination of the conformation of the template compound is one of the critical steps in 3D QSAR studies. Conformational properties of 12 as it is mentioned above were studied previously by our group using a combination of 1D, 2D NMR spectroscopy and molecular modeling techniques. Extended conformational analysis studies showed that, C3 alkyl side chain orients perpendicular to the ring system (conformer I in Figure 11) [59]. The knowledge of the receptor structure is not a prerequisite for 3D QSAR analysis, however, the availability of its crystal structure or 3D model facilitates the structure alignment, and can provide statistically more reliable models [60, 61]. The receptor model of the CB1 receptor obtained by Tuccinardi *et al.* [62], was complexed with the low energy conformers of 12. Low energy conformers of 12 were obtained using a Monte Carlo (MC) conformational search analysis.

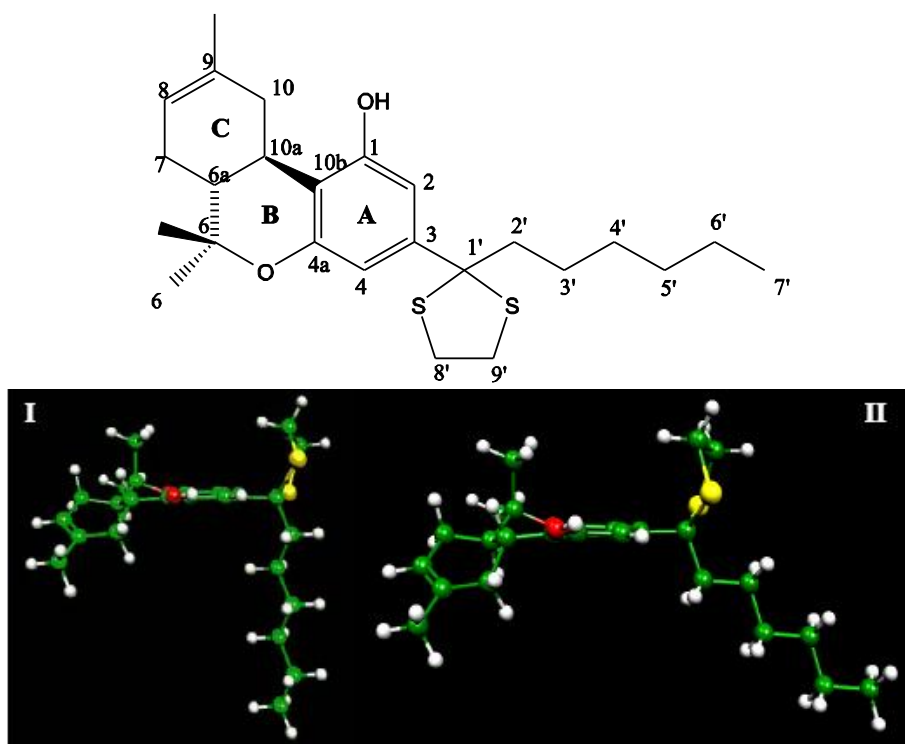


Figure 11. Molecular structure of 12 (above) and its conformers (below): conformer I derived from a combination of molecular modeling and experimental NMR spectroscopy, and conformer II derived from a combination of molecular modeling and molecular docking studies.

Flexible docking has been employed to the lowest energy conformers of 12 using the FlexX docking algorithm of SYBYL molecular modeling package [63]. FlexX is a docking method that uses an efficient incremental construction algorithm in order to optimize the interaction between a flexible ligand and rigid binding site residues of a receptor. Population

analyses of docking results showed that conformer II (Figure 11) had the highest percentage of conformation in the active site of receptor. Thus, we examined conformers I and II of compound 12 as a template ligand at the 3D QSAR analyses.

The CB1 receptor has two available sites (S1 and S2) for accommodating CB ligands (Figure 12). (i) S1 site; contains a cavity with a ~ 7 Å depth and accommodates the alkyl chain segment of the CB analogue. Our findings are in accordance with previous observations which show that extension of five carbon atom chain of THC by one or two carbon atoms (optimum alkyl chain length is ~ 7 Å) improves binding, while further extension (>7 Å) is detrimental due to steric hindrance (ii) S2 site; contains a cavity with a ~ 10 Å depth and accommodates the alkyl chain segment of the CB ligand.

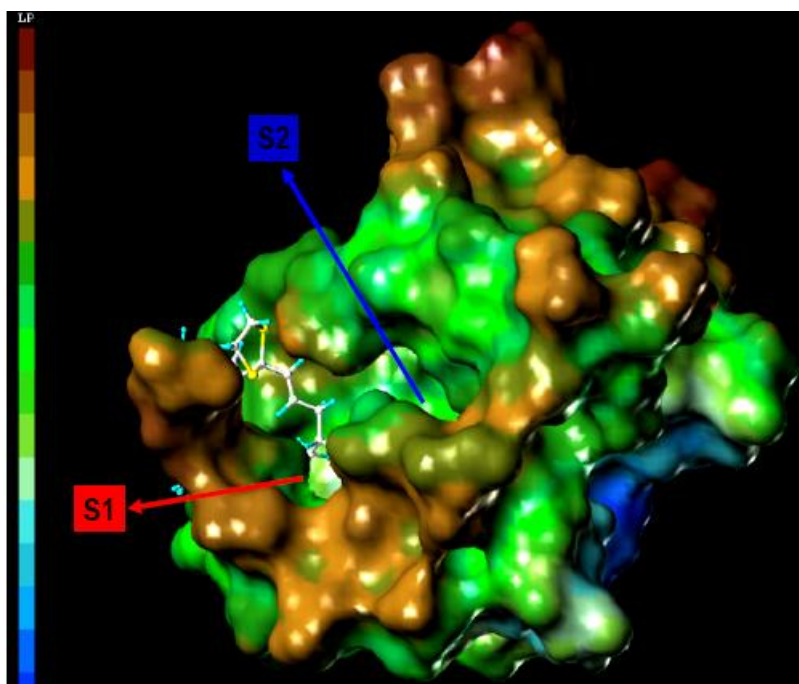


Figure 12. Two cavities S1 and S2 are observed at the active site of the CB1 receptor: (i) S1 site; contains a cavity with a ~ 7 Å depth and accommodates alkyl chain segment of CB ligand. (ii) S2 site; contains a cavity within a ~ 10 Å depth and accommodates alkyl chain segment of CB (LP: Lipophilicity map; lipophilicity decreases from top to bottom).

Steric-electrostatic CoMSIA contour maps of 12, and its corresponding CBD analogue 13 have been showed for the CB1 receptor using the template ligand as conformer I of 12 (Figures 13a. and 13b.). Steric-electrostatic CoMSIA contour maps of 12, and its corresponding CBD analogue 13 have been represented for the CB1 receptor using the template ligand as conformer II of 12 (Figures 13c. and 13d.). The individual contributions from the steric and electrostatic favored and disfavored levels are fixed at 80% and 20%, respectively. The CoMSIA contours of the steric maps are shown in yellow and green colors, and those of the electrostatic contour maps are shown in red and blue colors. Greater values of “bioactive measurement” are collected with: Bulky groups near the green colored contours; not bulky groups near the yellow

colored contours; more positive charge near the blue colored contours, and more negative charge near the red colored contours.

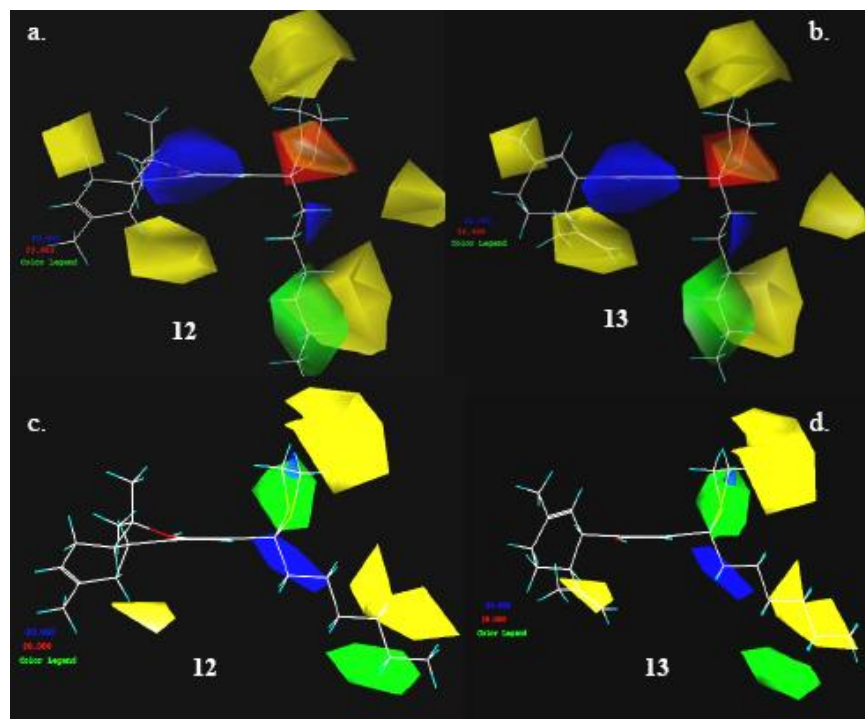


Figure 13a. CoMSIA contour maps of 12, b. and its corresponding CBD analogue 13 when conformer I was used as template, c. CoMSIA contour maps of 12, and d. corresponding CBD analogue 13 when conformer II was used as template. Sterically favored areas are shown in green color (contribution level of 80%). Sterically unfavored areas are shown in yellow color (contribution level of 20%). Positive potential favored areas are shown in blue color (contribution level of 80%). Positive potential unfavored areas are shown in red color (contribution level of 20%).

Three general conclusions could be drawn from the characteristics of derived 3D contour maps of CoMSIA models using both conformations of template ligand 12:

- Steric effects determine the binding affinity. The relative contributions of steric fields are larger than the electrostatic fields.
- The orientation of the C3-alkyl chain plays a crucial role in determining the biological activity. The green colored contours along the left side of the end of the alkyl chain (corresponding to shown snapshot contour plots, Figure 13) show that bulky groups enhance the binding affinity, whereas bulky groups in the right sides of the C3-alkyl chain of analogues lead to decreased binding affinity.
- Because of the structural differences of Δ^8 -THC and CBD derivatives at the cyclic ring segment, these groups have different pharmacophoric requirements for their receptors in these regions. While sterically unfavorable areas are located on the methyl or propenyl groups of CBD analogues, these unfavorable regions are located at the

vicinity of the tricyclic segment of Δ^8 -THC analogues (Figure 13). Therefore, Δ^8 -THC analogues have higher binding affinities than their corresponding CBD analogues.

The conformers I and II of 12 used as a template compound in CoMSIA analyses show similarities and differences in contour maps. Their similarities are reflected in the same regions that contour levels of identical color cover. However, close observation reveals significant differences in their shape and extent of covering of the contour regions. The conformational differences of conformers I and II are localized in the alkyl chain. Our results confirm the earlier literature reports that the lipophilic alkyl chain plays crucial role in determining cannabimimetic activity for the CB1 receptor. Thus, the differences of contour maps at alkyl chain are important for the interpretation of pharmacophore groups that affect the binding affinity. When conformer I is used as a template, both THC and CBD analogues have green colored contour (depicts sterically favorable groups) at the tail of alkyl chain (on top of Figure 13). However, if conformer II is used as a template compound, then at the tail of alkyl chain only THC fits green colored contour (on bottom-left of Figure 13). CBD analogues do not fit green colored contours but they fit yellow colored contours (depicts sterically unfavorable groups) (on bottom-right of Figure 13). These important observations are obtained only by the model that was constructed on conformer II of 12. The contour plots at the tail of alkyl chain which derived by the model that constructed on conformer II of 12 demonstrates the better binding affinity of THC analogues than the corresponding CBD analogues.

Conformer I of 12 fits the S1 site of the receptor, whereas conformer II of 12 fits the S2 site of the receptor. More clearly seen in Figure 12, the S1 site has more lipophilic character than the S2 site. Unsaturation of the alkyl chain leads its orientation towards the S2 site. For this reason an analogue of 12 was designed possessing four unsaturated bonds which were directed specifically to the S2 cavity. The proposed molecule will be synthesized and tested for its biological activity in order to validate our rational design. Depending on the observed activity we will be able to differentiate if optimum activity is induced by S1 or S2 sites. These observations may help open new avenues to synthetic chemists for synthesizing novel compounds.

In conclusion, we applied a novel approach to generate new structures aiding in the rational drug design. This approach is based on the combination of theoretical calculations, molecular docking and 3D QSAR studies. Such an approach appears to be superior to the 3D QSAR results, previously reported by our group, using a combination of theoretical calculations and NMR spectroscopy. Figure 14 describes the overall procedure using a flowchart. It is therefore advised when the crystal structure of a 3D model of a receptor is known, to use the conformation of the template derived from the combination of theoretical calculations and ranking of docking scores, as well as population analysis of docked conformers. It is well known that the knowledge of the receptor structure is not a prerequisite for 3D QSAR analysis, however, this study clearly shows that the availability of a crystal structure or 3D model for a receptor facilitates the structure alignment and provides a model marginally more reliable statistically.

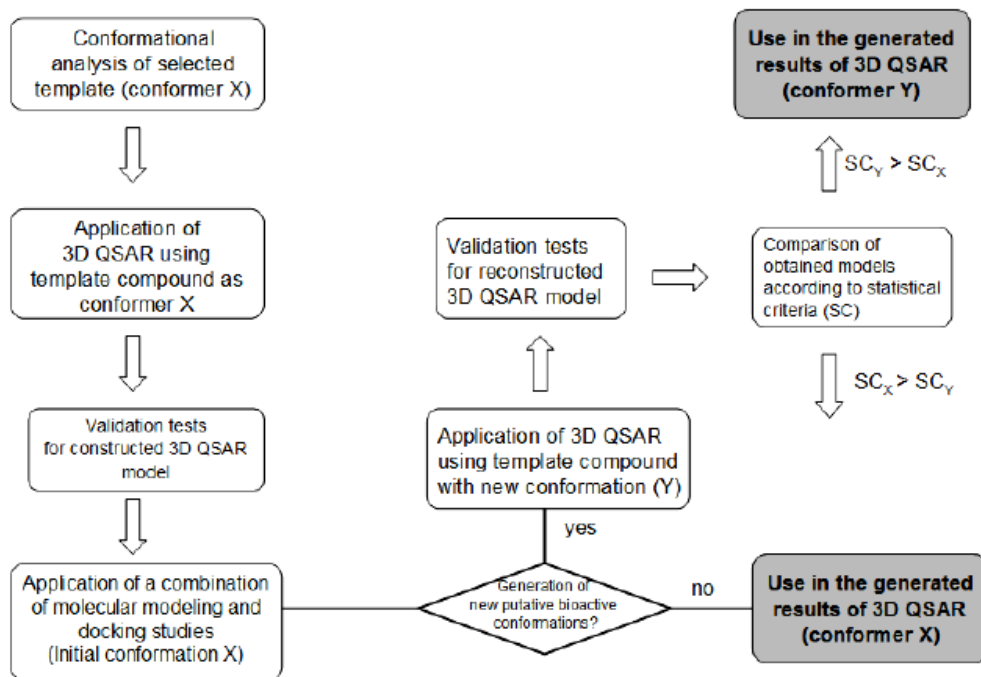


Figure 14. Flow chart showing the comparative steps used in the analysis of data derived through a combination of molecular modeling and NMR experiments with molecular modeling and docking results.

We are currently studying the interactions of the cannabinoids in more simulating biological environments (for example the active site of the receptor is not kept rigid and it is associated with lipid bilayer environment).

Conformational Analysis of Linear and Cyclic Peptides

Multiple sclerosis (MS) is a progressive demyelinating disease of the central nervous system (CNS) in which a coordinated attack of the immune system takes place against the myelin sheath [64]. Although the antigenic components of myelin in MS have not been identified with certainty yet, myelin basic protein (MBP) is believed to be one of the main candidate autoantigens, and MBP87-99 is encephalitogenic in experimental autoimmune encephalomyelitis (EAE), the best studied animal model for MS [65-69].

Analogs of immunodominant epitopes of these proteins (altered peptide ligands, APLs) can induce or suppress EAE in rodents through the formation of a trimolecular complex between the major histocompatibility complex (MHC)-peptide (antigen)-T-cell receptor (TCR) and the triggering of different immunological responses. Antagonism requires an APL to induce biochemical activity, which is inhibitory over the agonist delivered signals.

A two-step mechanism for TCR recognition has been proposed [70]. Initial TCR-MHC interactions guide the TCR to its ligand in an orientation that positions the rigid CDR1 and

CDR2 loops mainly over the MHC. This is followed by a final folding of the two highly flexible CDR3 loops [71] of the TCR over the peptide. T-cell activation is triggered only on the formation of stable peptide contacts, and APLs induce biochemical activity which is inhibitory over the agonist-delivered signals. Thus, the TCR may scan MHC molecules using a “lock and key” type of binding with its CDR1 and CDR2 loops, followed by an induced fit of its CDR3 loops over the peptide [72].

X-ray studies have shown that the TCR from human autoimmune disease binds to the peptide-HLA-DR2b complex with an off-center mechanism, which positions the CDR3 loops of the TCR over residues His88 and Phe89 of the N-terminus of the MBP85-98 epitope [73]. It is one of the best characterized TCRs from a human autoimmune disease, and this aberrant binding mode provides a possible explanation for the fact that in MS autoreactive T-cells escape deletion in the thymus and attack self-myelin. Similarly, the trimolecular complex of TCR-peptide-HLA-DR2a [74] reveals that the TCR primarily recognizes the N-terminal portion of MBP peptide too.

The rational design of APLs, which inactivate autoreactive specific T-cells, appears as a promising strategy in the treatment of MS. These APLs could bind with high affinity with MHC and compete for recognition of self-antigens at the antigen presentation, without activating disease-causing T-cells. Indeed, linear APLs [Arg⁹¹, Ala⁹⁶]MBP87-99 and [Ala^{91,96}]MBP87-99, which have critical TCR substitutions, have been shown to inhibit EAE induced by the guinea pig MBP74-85 epitope in Lewis rats [75-77]. The use of linear peptides in therapeutic protocols, though, is limited because of their proteolytic degradation. However, such linear peptides can be the lead compounds for a rational design of cyclic molecules and finally peptide mimetics or non-peptide mimetics.

Hereby, we outline the strategy applied for Conformational Analysis of linear [78, 79] and cyclic peptides [80-82] and how this is related to the drug design and synthesis of novel potential therapeutic analogs.

Linear peptides are very flexible entities, with a considerable number of degrees of freedom. The main problem in analysis of NOEs and their application in conformational analysis is the averaging of NOEs. In addition, analysis of the NMR spectra of such entities is not straightforward due to the observed severe overlap of the peaks, and it becomes more difficult the longer the peptide is. The overlap deteriorates especially when an amino acid appears in the amino sequence more than once. Figure 15 presents such a NOESY spectrum, for the 13-amino acid long peptide [Arg⁹¹, Ala⁹⁶]MBP₈₇₋₉₉. The overlapping not only makes the identification a difficult task but also means that the number of meaningful NOEs is limited. However, the major problem is not the overlapping in analysis.

In this case, we follow a strategy of conformational analysis including a combination of unrestrained and backbone restrained molecular dynamics simulations. All the resulting conformations are scanned for compliance with the NMR derived distances. The aim is not to calculate the average structure that complies with all NOEs and does not represent the real situation in solution, but instead, to shed light into the whole conformational ensemble. Such approach reveals many energetically favored conformations and agrees with the general accepted concept that peptides bind to their receptor in a low energy conformation, not necessarily the global minimum.

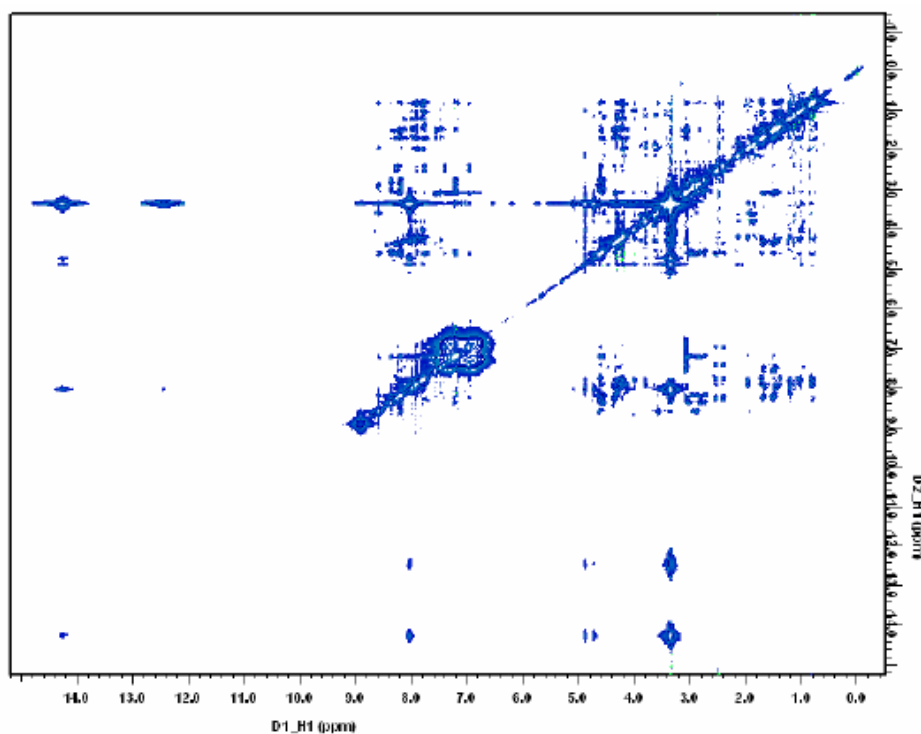


Figure 15. NOESY spectrum of $[\text{Arg}^{91}, \text{Ala}^{96}] \text{MBP}_{87-99}$ in $\text{DMSO-}d_6$ recorded on a Varian INOVA 600 MHz spectrometer.

Three sets of MD runs are performed. The first set of dynamics is completely unrestrained, while the remaining two sets are backbone restrained. Backbone distance constraints are employed to allow enough freedom to the side chains, so that sufficient sampling of conformational space could be obtained. Upper and lower bounds are used to establish a target interval.

Sequential NH-NH distance constraints are used in the first set, in an attempt to obtain conformations within the α_L region of the Ramachandran map, and sequential $\text{H}\alpha$ -NH constraints are used in the second set, for sampling of the β region. All resulting conformations are subjected to a completely unrestrained energy minimization, in order to make a direct comparison with the NMR results. The final ensemble is checked so that the structures have backbone dihedral angles φ and ψ within the core region of the Ramachandran map, and *trans* ω dihedral angles. Virtual dihedral angle ζ is also examined, to evaluate the planarity of C_α .

The selected low energy structures are grouped into families according to their backbone dihedral angles and overall RMSD (in Å) when compared to the lowest energy structure of each run. All clusters are examined for consistency with experimental distance information designated by the obtained NOEs. Thus, populations of various conformers that represent local minima at the potential energy surface are identified.

The methodology described was followed for the linear altered peptide ligands (APLs) $[\text{Ala}^{91,96}] \text{MBP}_{87-99}$ and $[\text{Arg}^{91}, \text{Ala}^{96}] \text{MBP}_{87-99}$ in order to generate a set of conformers that are in accordance with the most critical NOEs, representing the true flexibility of the APLs. In each case a unique conformation was proposed as active. The aim of the work was to correlate

the linear peptides' antagonistic activity with the 3D conformation they adopt. The linear peptides [Ala^{91,96}] MBP₈₇₋₉₉ and [Arg⁹¹, Ala⁹⁶] MBP₈₇₋₉₉ were chosen to be studied as a basis to derive useful conclusions, which will consecutively be applied to design cyclic peptides or mimetics.

The detailed conformational analysis of the APLs led to the identification of a common structural motif, as derived from superimposition of both proposed putative active conformations (Figure 16). These conformations were chosen as potential bioactive since they had the least RMSD value compared to the native docked MBP82-97 from X-ray crystallographic data. Major histocompatibility complex (MHC) anchor residues have to be in a certain spatial arrangement, with their side chains available to interact with the receptor. T-cell receptor (TCR) contact residue Phe⁸⁹ presents a different behavior, though: it seems that the antagonistic activity of the APLs may be due to the loss of some hydrophobic interactions with the T-cell receptor, caused by the altered topology of the phenyl side chain with respect to the native peptide as found via crystallography.

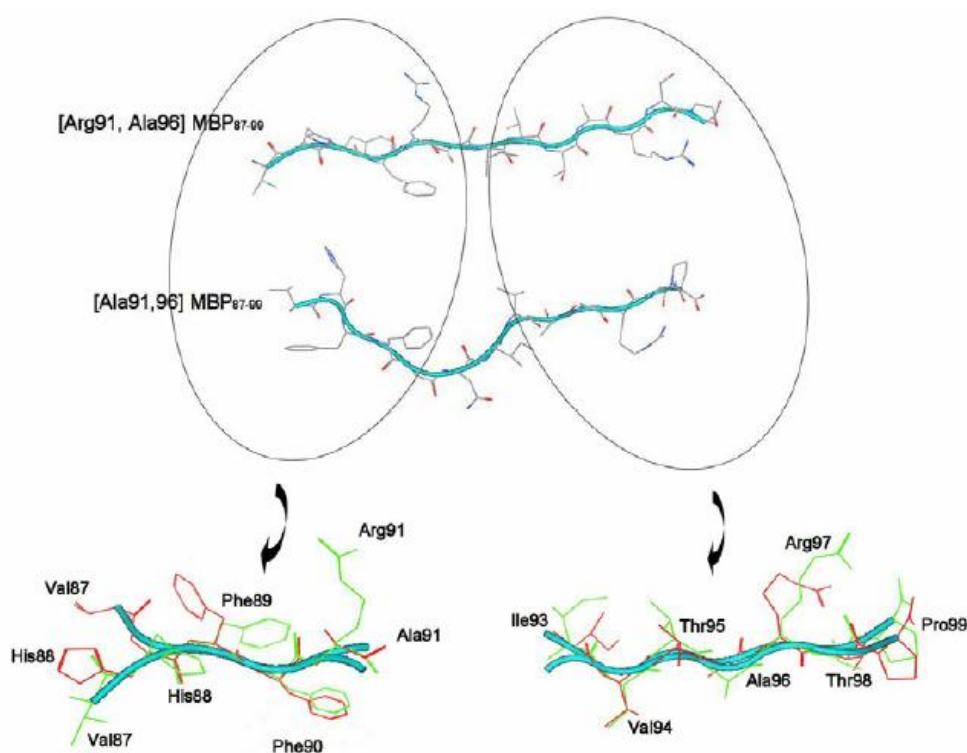


Figure 16. Two different superimpositions between the proposed putative bioactive conformations of [Arg⁹¹, Ala⁹⁶] MBP₈₇₋₉₉ (green) and [Ala^{91,96}] MBP₈₇₋₉₉ (red). The backbone of both peptides is represented as a cartoon. Residues 88-90 (left - C_α RMSD is 0.21 Å) and residues 93-98 (right - C_α RMSD is 0.88 Å). Despite the difference, caused by the substitution of Arg⁹¹ with Ala⁹¹, the distance between primary MHC anchors Val⁸⁷ and Phe⁹⁰ remains relatively stable in both molecules: d_{Cβ-Cβ} (Val⁸⁷-Phe⁹⁰) is 10.83 Å in [Arg⁹¹, Ala⁹⁶] MBP₈₇₋₉₉ and 11.31 Å in [Ala^{91,96}] MBP₈₇₋₉₉. The same distance is 10.80 Å in the native peptide.

Two EAE antagonist cyclic analogues cyclo(87-99) [Arg91, Ala96] MBP87-99 and cyclo(87-99) [Ala91,96] MBP87-99 have been designed and synthesized. These molecules are as active against EAE induced by guinea pig MBP72-85 epitope as their linear counterparts, but they present enhanced stability. Acute monophasic EAE was developed in Lewis rats with guinea pig MBP72-85 alone, while EAE development was completely prevented by the co-administration of cyclo(87-99) [Arg91, Ala96] MBP87-99 and cyclo(87-99) [Ala91,96] MBP87-99. Tissue samples from Lewis rats injected with MBP72-85 in complete adjuvant showed mononuclear cells around small vessels of the spinal cord. On the other hand, no inflammation was observed in any spinal cord sample from the Lewis rats immunized with cyclo(87-99) [Arg91, Ala96] MBP87-99 and cyclo(87-99) [Ala91,96] MBP87-99 alone or co-injected with agonist MBP72-85 and antagonist APLs. The cyclic peptides were found to be more stable to lysozymal enzymes and Cathepsin B, D, and H, compared to their linear counterparts. Moreover, cyclo(87-99) [Arg91, Ala96] MBP87-99 and cyclo(87-99) MBP87-99 were found to decrease the Th2/Th1 ratio in peripheral blood mononuclear cells (PBMC) from MS patients and bound with comparable affinity to HLA-DR4.12 Cyclo(87-99) MBP87-99 only induced weak EAE clinical signs in Lewis rats (clinical score 1) and affected T-cell (CD4+ T-cell line derived from an MS patient) proliferation.¹² The antagonist cyclic peptide, cyclo-(87-99) [Arg91, Ala96] MBP87-99, inhibited proliferation of the in vitro generated CD4+T-cell clone (specific for MBP87-99).

Cyclic peptides, by definition, have a more restricted backbone conformational space. Even if the amount of meaningful NOEs is not satisfying, distance geometry calculations are followed to investigate the low energy conformers complying with the experimental distances. The NOE-derived structural information extracted from the analysis of NOESY spectra acquired in solutions is introduced to DYANA software for structure calculation. The family ensemble of 20 best DYANA models (out of 400 calculated) in terms of target function ($<0.4 \text{ \AA}^2$) and NOE violations ($<0.2 \text{ \AA}$), is refined through REM (AMBER 5.0; SANDER program). A force constant of $133.76 \text{ kJ mol}^{-1} \text{ \AA}^2$ is applied for the distance constraints. The mean conformations of the APLs cyclo(87-99) MBP87-99, cyclo(87-99) [Ala91,96] MBP87-99, and cyclo(87-99) [Arg91, Ala96] MBP87-99 are shown in Figure 17.

The obtained results show that the two antagonist cyclic APLs form a bend in the middle segment of their sequence, leading to structures that are more compact, with a smaller solvent accessible area. Thus, they do not occlude weak interactions with an approaching TCR and can cause EAE antagonism. In contrast, cyclo(87-99) MBP87-99 is more compact in the NH terminus of the molecule but presents an overall larger solvent accessible area, which may block the approach of a TCR and prevent either an agonistic or an antagonistic action. Representation of their MBP linear and cyclic APLs with MHC are shown in Figure 18.

Proposal of a Pharmacophore Model. The NMR analysis identified structural data which may be combined and led to the establishment of a pharmacophore model for APLs presenting EAE antagonism. MOE 2006.08 25 was used for the generation of the pharmacophore model. An essential characteristic for EAE antagonism is the formation of weak interactions between the bimolecular complex APL-MHC with the T-cell receptor.

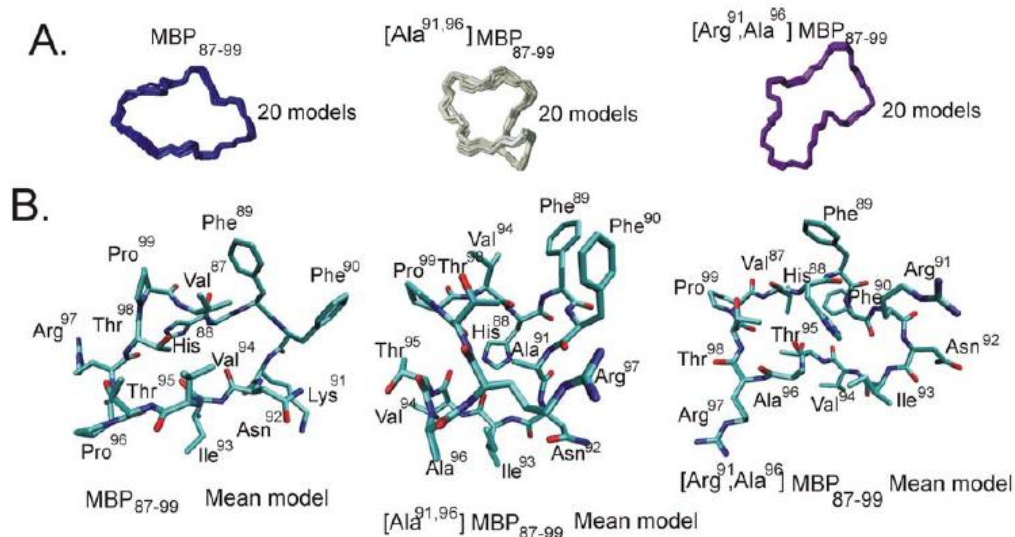


Figure 17. (A) The family of 20, energy minimized, DYANA models calculated for the cyclo (87-99) MBP₈₇₋₉₉, cyclo (87-99) [Ala^{91,96}]MBP₈₇₋₉₉ and cyclo (87-99) [Arg⁹¹,Ala⁹⁶]MBP₈₇₋₉₉ analogues, respectively and (B) the mean energy minimized cyclo (87-99) MBP₈₇₋₉₉, cyclo (87-99) [Ala^{91,96}]MBP₈₇₋₉₉ and cyclo (87-99) [Arg⁹¹,Ala⁹⁶]MBP₈₇₋₉₉ structures, respectively. Figures were generated with the MOLMOL program.

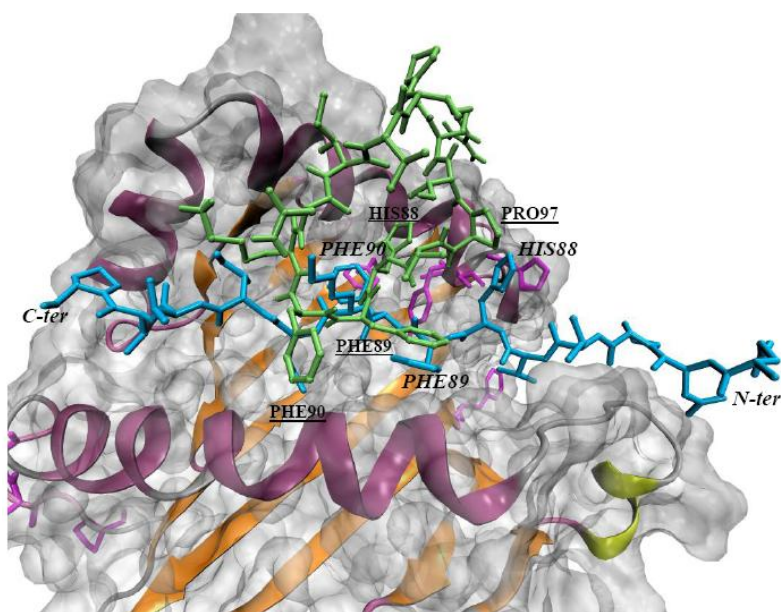


Figure 18. Representation of the cyclo(87-99) MBP₈₇₋₉₉-MHC model complex. MHC is shown as a cartoon representation, and the cyclo(87-99) MBP₈₇₋₉₉ docked peptide is shown as green. For comparison, the linear peptide MBP₈₅₋₉₈ is shown at its crystallographic position as cyan. The DRb aminoacids of MHC are shown as purple. His⁸⁸, Phe⁸⁹, and Phe⁹⁰ of both cyclo (underlined) and linear (italicic) peptide are labeled.

Structural data from the analysis of cyclo(87-99) MBP87-99 suggest that the lack of bioactivity might be due to the overall bulky orientation of the APL over the MHC molecule, which prevents any subsequent binding of the TCR. Therefore, the first feature in the proposed pharmacophore model is the exclusion volume V1 (Figure 19).

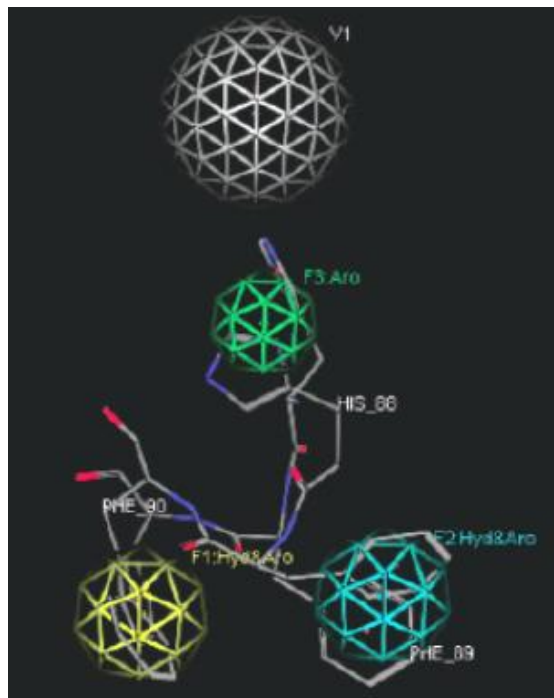


Figure 19. Pharmacophore model generated by the structural data obtained from the conformational analysis for the cyclic APLs. Exclusion volume V1 is presented with a gray sphere, feature F1 (Phe90) with a yellow sphere, F2 (Phe89) with cyan, and F3 (Phe88) with a green sphere.

The radius of the sphere is 2.8 Å. The second feature F1 is located in the region of the phenyl ring of Phe90. The center of the sphere in this case lies on the virtual line connecting the centroids of the ring in the conformations of the two antagonistic APLs, while the radius is 1.9 Å, creating a volume big enough to accommodate a hydrophobic and aromatic ring. The same procedure has been followed for the third feature F2, for which the center is placed on the virtual line connecting the centroids of the phenyl ring of Phe89 in cyclo(87-99) [Arg91, Ala96] MBP87-99 and cyclo(87-99) [Ala91,96] MBP87-99.

The sphere should again be occupied by a hydrophobic and aromatic ring, selecting a radius of 1.9 Å for the reason mentioned above. The last feature in the pharmacophore model, F3, was once more chosen to be generated where the imidazole ring of His88 lies in the two APLs. The radius of the sphere is once again 1.9 Å, and the desired characteristic this time is occupation by an aromatic group. The pharmacophore model defined in this study contains information regarding MHC (Phe90) and TCR anchors (His88, Phe89) as well as the overall volume of the target molecules that should not occlude weak interactions with an approaching TCR and therefore may suppress EAE antagonism.

NMR shows that among the three peptides the proximity of residues in positions 91 and 97 is favorable only in cyclo(87-99) [Ala91,96] MBP87-99. When Ala is replaced by Lys91/Arg91 in cyclo(87-99) MBP87-99 and in cyclo(87-99) [Arg91, Ala96] MBP87-99, respectively, no NOE between the long, positively charged Lys91/Arg91 side chain and that of Arg97 is observed. In these cases, charge repulsion between Lys91/Arg91 and Arg97 seems to account for the orientation of Lys/Arg and Arg97 side chains toward opposite directions. In cyclo(87-99) [Arg91,Ala96] MBP87-99, though, there is a β II turn formed in the sequence 92-96, a feature which is not present in cyclo(87-99) MBP87-99. This conformational characteristic is responsible for the more compact conformations of the antagonist APLs, which in turn possibly allows the TCR to approach, form weak interactions with the pMHC, and induce biochemical activity which is inhibitory over the agonist-delivered signals.

The design and synthesis of cyclic peptide analogues is the most important step in the rational design of peptidomimetics or non-peptide mimetics. The conformational flexibility of a cyclic analogue is restricted, and the orientation of side chain groups important for binding could lead to the design of nonpeptide analogues. In this paper, based on the conformations of the studied cyclic analogues obtained from the NMR analysis, we proposed a pharmacophore model, which will be the first step toward the design and synthesis of organic molecules using rigid templates.

We have provided examples of the contribution of conformational analysis in three classes of molecules. First, the conformational analysis of AT₁ antagonists and superimposition studies with ANG II provided the design and synthesis of new analogs. Although these molecules are not as active as prototype losartan, they provide a new avenue for synthetic effort. Second, the conformational analysis of cannabinoids provided new information in their receptor subtypes and lead to the design of new analogs which are under evaluation in our synthetic program. Third, the conformational properties of MBP peptide epitopes modified through engineering their sequence and evaluated local structural variation due to these modifications have been studied. Obtained high-resolution 3D models of synthetic MBP peptides revealed the conformational differences and similarities between linear and cyclic APLS. Coupled with the known effect on their bioactivity, this could lead to the exploration of the molecular basis of EAE antagonism and the rational design of non-peptide mimetics.

References

- [1] Mavromoustakos, T; Zervou, M; Zoumpoulakis, P; Kyrikou, I; Benetis, NP; Polevaya, L; Roumelioti, P; Giatas, N; Zoga, A; Moutevelis Minakakis, P; Kolocouris, A; Vlahakos, D; Golic Grdadolnik, S; Matsoukas, J. Conformation and Bioactivity. Design and Discovery of Novel Antihypertensive Drugs. *Curr. Top. Med. Chem.* 2004, 4, 385-401.
- [2] Henry, G; Sykes, B. Strategies for the use of NMR spectroscopy in biological macromolecules and assemblies. *Bull. Can. Biochem. Soc.* 1987, 24, 21-26.
- [3] Burnier, M; Brunner, HR. Comparative antihypertensive effects of angiotensin II receptor antagonists. *J. Am. Soc. Nephrol.* 1999, 10, 12S, Suppl., S278-S282.

- [4] Pool, JL; Schmieder, RE; Azizi, M; Aldigier, JC; Januszewicz, A; Zidek, W; Chiang, Y, Satlin, A. Aliskiren, an orally effective rennin inhibitor, provides antihypertensive efficacy alone and in combination with Valsartan. *Am. J. Hypert.* 2007, 20, 11-20.
- [5] Wexler, RR; Greenlee, WJ; Irvin, JD; Goldberg, MR; Prendergast, K; Smith, RD; Timmermans, P.B.M.W.M. Non peptide Angiotensin II receptor antagonists: the next generation in antihypertensive therapy. *J. Med. Chem.* 1996, 39, 625-655.
- [6] Pantev, E; Stenman, E; Wackenfors, A; Edvinsson, L; Malmsjo, M. Comparison of the antagonistic effects of different angiotensin II receptor blockers in human coronary arteries. *Eur. J. Heart Fail.* 2002, 4, 699-705.
- [7] Garcha, RS; Sever, PS; Hughes, AD. Action of AT₁ receptor antagonists on angiotensin II-induced tone in human isolated subcutaneous resistance arteries. *Br. J. Pharmacol.* 1999, 127, 1876-1882.
- [8] Pelet, C; Mironneau, C; Rakotoarisoa, L; Neuilly, G. Angiotensin II receptor subtypes and contractile responses in portal vein smooth muscle. *Eur. J. Pharmacol.* 1995, 279, 15-24.
- [9] Zhang, JS; Van Meel, JC; Pfaffendorf, M.; Van Zwieten, PA. Different types of angiotensin II receptor antagonism induced by BIBS 222 in the rat portal vein and rabbit aorta; the influence of receptor reserve. *J. Pharmacol. Exp. Ther.* 1994, 269, 509-514.
- [10] De Gasparo, M; Catt, KJ; Inagami, T; Wright, JW; Unger, T. International Union of Pharmacology XXIII. The Angiotensin II Receptors. *Pharmacol. Rev.* 2000, 52, 415-472.
- [11] Plevaya, L.; Mavromoustakos, T.; Zoumboulakis, P.; Grdadolnik, SG.; Roumelioti, P; Giatas, N; Mutule, I; Keivish, T; Vlahakos, DV; Iliodromitis, EK; Kremastinos, DTh; Matsoukas, J. Synthesis and study of cyclic angiotensin II antagonist analogue reveals the role of $\pi^*-\pi^*$ interactions in the C-terminal aromatic residue for agonist activity and its structure resemblance with AT₁ non-peptide antagonists. *Bioorg. Med. Chem.* 2001, 9, 1639-1647.
- [12] Sakarellos, C; Lintner, K; Piriou, F; Femandjian, S. Conformation of the central sequence of angiotensin II and analogs. *Biopolymers* 1983, 22, 663-687.
- [13] Martin, J; Krum, H. Role of valsartan and other angiotensin receptor blocking agents in the management of cardiovascular disease. *Pharmacol. Res.* 2002, 46, 203-212.
- [14] Mavromoustakos, T; Kolocouris, A; Zervou, M; Roumelioti, P; Matsoukas, J; Weisemann, R. An effort to understand the molecular basis of hypertension through the study of conformational analysis of losartan and sarmesin using a combination of Nuclear Magnetic Resonance spectroscopy and theoretical calculations. *J. Med. Chem.* 1999, 42, 1714-1722.
- [15] Mavromoustakos, T; Kapou, A; Benetis, NP; Zervou M. Conformational analysis using 2D NMR spectroscopy coupled with computational analysis as an aid in the alignment procedure of 3D-QSAR studies. *Drug Des. Rev. Online* (2004).
- [16] Chiolero, A; Burnier, M. Pharmacology of valsartan, an angiotensin II receptor antagonist. *Expert Opin. Invest. Drugs* 1998, 7, 1915-1925.
- [17] De Gasparo, M; Whitebread, S. Binding of valsartan to mammalian angiotensin AT₁ receptors. *Regul. Pept.* 1995, 59, 503-511.

- [18] Fogari, R; Zoppi, A; Mugellini, A; Preti, P; Banderali, A; Pesce, RM; Vanasia, A. Comparative efficacy of losartan and valsartan in mild-to-moderate hypertension. *Curr. Ther. Res.* 1999, 60, 195-206.
- [19] Shetty, SS; Delgrande, D. Differential Inhibition of the Prejunctional Actions of Angiotensin II in Rat Atria by Valsartan, Irbesartan, Eprosartan and Losartan. *J. Pharm. Exper. Therap* 2000, 294, 179-186.
- [20] Hedener, T; Oparil, S; Rasmussen, K; Rapelli, A; Gatlin, M; Kobi, P; Sullivan, J; Oddou-Stock, P. A comparison of the angiotensin II antagonists valsartan and losartan in the treatment of essential hypertension. *Am. J. Hyper.* 1999, 12, 414-417.
- [21] Mistry, NB; Westheim, AS; Kjeldsen, SE. The angiotensin receptor antagonist valsartan: a review of the literature with a focus on clinical trials. *Exp. Opin. Pharmacotherapy* 2006, 7, 575-581.
- [22] Chrysant, SG; Chrysant, GS. Clinical experience with angiotensin receptor blockers with particular reference to valsartan. *J. Clin. Hypertens.* 2004, 6, 445-451.
- [23] Kjeldsen, SE; Julius, S; Arbor, A. Hypertension mega-trials with cardiovascular end points: Effect of angiotensin-converting enzyme inhibitors and angiotensin receptor blockers. *Am. Heart J.* 2004, 148, 747-754.
- [24] Manabe, S; Okura, T; Watanabe, S; Fukuoka, T; Higaki, J. Effects of angiotensin II receptor blockade with valsartan on pro-inflammatory cytokines in patients with essential hypertension. *J. Cardiovasc. Pharmacol.* 2005, 46, 735-739.
- [25] Moutevelis-Minakakis, P; Gianni, M; Stougiannou, H; Zoumpoulakis, P; Zoga, A; Vlahakos, AD; Iliodromitis, E; Mavromoustakos, T. Design and Synthesis of Novel Antihypertensive Drugs *Bioorg. Med. Chem. Lett.* 2003, 13, 1737-1740.
- [26] Mavromoustakos, T; Moutevelis-Minakakis, P; Kokotos, CG; Kontogianni, P; Politi, A; Zoumpoulakis, P; Findlay, J; Cox, A; Balmforth, A; Zoga, A, Iliodromitis, E. Synthesis, binding studies, and in vivo biological evaluation of novel non-peptide antihypertensive analogs. *Bioorg. Med. Chem* 2006, 14, 4353-4360.
- [27] Mavromoustakos, T; Zervou, M; Zoumpoulakis, P. Design and discovery of novel antihypertensive drugs through conformation and bioactivity studies. In Co-Editors: Attatur-Rahman, Allen B. Reitz. Associate Editors: M. Iqbal Choundhary, Cheryl P. Kordik. Ur. *Frontiers in Medicinal Chemistry: Cardiovascular Diseases.* The Netherlands: Bentham Science Publishers Ltd.; 2006; 3, 87-113.
- [28] Gaoni, Y; Mechoulam, R. Isolation, structure and partial synthesis of an active constituent of hashish. *J. Am. Chem. Soc.* 1964, 86, 1646-1647.
- [29] Devane, WA; Dysarz, FA; Johnson, MR; Melvin, LS; Howlett, A. C. Determination and characterization of a cannabinoid receptor in rat brain. *Mol. Pharmacol.* 1988, 34, 605-613.
- [30] Munro, S; Thomas, KL; Abu-Shar, M. Molecular characterization of a peripheral receptor for cannabinoids. *Nature* 1993, 365, 61-65.
- [31] Reggio, P. H. Pharmacophores for ligand recognition and activation/inactivation of the cannabinoid receptors *Curr. Pharm. Des.* 2003, 9, 1607-1633.
- [32] Herkenham, M; Lynn, AB; Little, MD; Johnson, MR; Melvin, LS; De Costa, BR; Rice, KC. Cannabinoid Receptor Localization in Brain. *Proc. Natl. Acad. Sci. USA.* 1990, 87, 1932-1936.

- [33] Straiker, AJ; Maguire, G; Makie, K; Lindsey, J. Localization of cannabinoid CB1 receptors in the human anterior eye and retina. *Invest Ophthalmol. Visual. Sci.* 1999, 40, 2442–2448.
- [34] Thakur, GA; Duclos Jr, RI; Makriyannis, A. Natural cannabinoids: Templates for drug discovery. *Life Sci.* 2005, 78, 454-466.
- [35] Fichera, M; Cruciani, G; Bianchi, A; Musumarra, G. 3D-QSAR study on the structural requirements for binding to CB(1) and CB(2) cannabinoid receptors. *J. Med. Chem.* 2000, 43, 2300-2309.
- [36] Khanolkar, AD; Palmer, SL; Makriyannis, A. Molecular probes for the cannabinoid receptors. *Chem. Phys. Lipids* 2000, 108, 37-52.
- [37] Galiegue, S; Mary, S; Marchand, J; Dussossoy, D; Carriere, D; Carayon, P; Bouaboula, M; Shire D; Le Fur, G; Casellas, P. Expression of central and peripheral cannabinoid receptors in human immune tissues and leukocyte subpopulations. *Eur. J. Biochem.* 1995, 232, 54–61.
- [38] Oz, M. Receptor-independent actions of cannabinoids on cell membranes: Focus on endocannabinoids. *Pharmacol. Therapeut.* 2006, 111, 114-144.
- [39] Parkkari, T; Savinainen, JR; Raitio, KH; Saario, SM; Matilainen, L; Sirvio, T; Laitinen, JT; Nevalainen, T; Niemi, R; Jarvinen, T. Synthesis, cannabinoid receptor activity, and enzymatic stability of reversed amide derivatives of arachidonoyl ethanolamide. *Bioorg. Med. Chem.* 2006, 14, 5252-5258.
- [40] Salo, OMH; Savinainen, JR; Parkkari, T; Nevalainen, T; Lahtela-Kakkonen, M; Gynther, M; Laitinen, JT; Jarvinen, T; Poso, Antti. 3D-QSAR studies on cannabinoid CB1 Receptor Agonists: G-protein activation as biological data. *J. Med. Chem.* 2006, 49, 554-566.
- [41] Lambert, DM; Fowler, CJ. The endocannabinoid system: Drug targets, lead compounds, and potential therapeutic applications. *J. Med. Chem.* 2005, 48, 1-29.
- [42] Felder, CC Endocannabinoids and their receptors as targets for treating metabolic and psychiatric disorders. *Drug Discovery Today: Therapeutic Strategies* 2006, 3, 561-567.
- [43] Razdan, R. K. Structure-activity relationships in cannabinoids. *Pharmacol. Rev.* 1986, 38, 75-149.
- [44] Makriyannis, A; Rapaka, RS. The molecular basis of cannabinoid activity *Life Sci.* 1990, 47, 2173-2184.
- [45] Mavromoustakos, T; Theodoropoulou, E; Zervou, M; Kourouli, T; Papahatjis, D. Structure elucidation and conformational properties of synthetic cannabinoids (-)-2-(6a,7,10,10a-tetrahydro-6,6,9-trimethyl-1-hydroxy-6H-dibenzo[b,d]pyranyl)-2-hexyl-1,3-dithiolane and its methylated analog. *J. Pharm. Biomed. Anal.* 1999, 18, 947-956.
- [46] Keimowitz, AR; Martin, BR; Razdan, RK; Crocker, PJ; Mascarella, SW; Thomas BF. QSAR analysis of Δ^8 -THC analogues: Relationship of side-chain conformation to cannabinoid receptor affinity and pharmacological potency *J. Med. Chem.* 2000, 43, 59-70.
- [47] Shire, D; Calandra, B; Delpech, M; Dumont, X; Kaghad, M; Le Fur, G; Caput, D; Ferrara, P. Structural features of the central cannabinoid CB1 receptor involved in the binding of the specific CB1 antagonist SR 141716A. *J. Biol. Chem.* 1996, 271, 6941-6946.

- [48] Reggio, PH; Panu, AM; Miles, S. Characterization of a region of steric interference at the cannabinoid receptor using the active analogue approach. *J. Med. Chem.* 1993, 36, 1761-1771.
- [49] Semus, SF; Martin, BR. A computer graphic investigation into the pharmacological role of the THC-cannabinoid phenolic moiety. *Life Sci.* 1990, 46, 1781-1785.
- [50] Shim, JY; Collantes, ER; Welsh, WJ; Subramaniam, B; Howlett, AC; Eissenstat, MA; Ward, SJ. Three-dimensional quantitative structure-activity relationship study of the cannabimimetic (Aminoalkyl)indoles using comparative molecular field analysis. *J. Med. Chem.* 1998, 41, 4521-4532.
- [51] Thomas, BF; Compton, DR; Martin, BR; Semus, SF. Modeling the cannabinoid receptor: a three-dimensional quantitative structure-activity analysis. *Mol. Pharmacol.* 1991, 40, 656-665.
- [52] Thomas, BF; Adams, IB; Mascarella, SW; Martin, BR; Razdan, RK. Structure activity analysis of anandamide analogues: relationship to a cannabinoid pharmacophore. *J. Med. Chem.* 1996, 39, 471-479.
- [53] Klebe, G; Abraham, U; Mietzner, T. Molecular similarity indices in a comparative analysis (CoMSIA) of drug molecules to correlate and predict their biological activity. *J. Med. Chem.* 1994, 37, 4130-4146.
- [54] Papahatjis, DP; Kourouli, T; Abadji, V; Goutopoulos, A; Makriyannis, A. Pharmacophoric requirements for the cannabinoid side chains: Multiple bond and C1'-substituted Δ^8 -Tetrahydrocannabinols. *J. Med. Chem.* 1998, 41, 1195-1200.
- [55] Papahatjis, DP; Nikas, SP; Kourouli, T; Chari, R; Xu, W; Pertwee, RG.; Makriyannis, A. Pharmacophoric requirements for the cannabinoid side chain. Probing the cannabinoid receptor subsite at C1'. *J. Med. Chem.* 2003, 46, 3221-3229.
- [56] Papahatjis, DP; Nahmias, VR; Andreou, T; Fan, P; Makriyannis A. Structural modifications of the cannabinoid side chain towards C3-aryl and 1',1'-cycloalkyl-1' cyano cannabinoids. *Bioorg. Med. Chem. Lett.* 2006, 16, 1616-1620.
- [57] Papahatjis, DP; Nikas, SP; Andreou, T; Makriyannis, A. A novel 1',1'-chain substituted Δ^8 -tetrahydrocannabinols. *Bioorg. Med. Chem. Lett.* 2002, 12, 3583-3586.
- [58] Gareau, Y; Dufrense, C; Gallant, M; Rochette, C; Sawyer, N; Slipetz, DM; Tremblay, N; Weech, PK; Metters, KM; Labelle, M. Structure activity relationships of tetrahydrocannabinol analogues on human cannabinoid receptor. *Bioorg. Med. Chem.* 1996, 6, 189-194.
- [59] Durdagi, S; Kapou, A; Kourouli, T; Andreou, T; Nikas, SP; Nahmias, VR; Papahatjis, DP; Papadopoulos MG; Mavromoustakos, T. The application of 3D-QSAR studies for novel cannabinoid ligands substituted at the C1' position of the alkyl side chain on the structural requirements for binding to cannabinoid receptors CB1 and CB2. *J. Med. Chem.*, 2007, 50, 2875-2885.
- [60] Mavromoustakos, T; Kapou, A; Benetis, NP; Zervou, M. Conformational Analysis using 2D NMR Spectroscopy Coupled with Computational Analysis as an Aid in the Alignment Procedure of 3D-QSAR Studies. *Drug Des. Rev.-Online*, 2004, 1, 235-245.
- [61] Durdagi, S.; Papadopoulos, M. G.; Papahatjis, D. P.; Mavromoustakos, T. Combined 3D QSAR and Molecular Docking Studies to Reveal Novel Cannabinoid Ligands with Optimum Binding Affinity. *Bioorg Med Chem. Lett.*, 2007, 17, 6754-6763.

- [62] Tuccinardi, T; Ferrarini, PL; Manera, C; Ortore, G; Saccomanni, G; Martinelli, A. Cannabinoid CB2/CB1 selectivity. Receptor modeling and automated docking analysis *J. Med. Chem.* 2006, 49, 984-994.
- [63] Sybyl molecular modeling software package, ver. 6.8., 2001, Tripos Inc., St Louis, MO 63144.
- [64] Prat, ET; Martin, R. The immunopathogenesis of MS. *J. Rehab. Res. Devel.* 2002, 39, 187-200.
- [65] Zamvil, SS; Steinman, L. The T lymphocyte in experimental allergic encephalomyelitis. *Annu. Rev. Immunol.* 1990, 8, 579-621.
- [66] Ota, K; Matsui, M; Milford, EL; Mackin, GA; Weiner, HL; Hafler, DA. T-cell recognition of an immunodominant myelin basic protein epitope in multiple sclerosis. *Nature* 1990, 346, 183-187.
- [67] Valli, A; Sette, A; Kappos, L; Oseroff, C; Sidney, J; Miescher, G; Hochberger, M; Albert, E. D; Adorini, L. Binding of myelin basic protein peptides to human histocompatibility leukocyte antigen class II molecules and their recognition by T cells from multiple sclerosis patients. *J. Clin. Invest.* 1993, 91, 616-628.
- [68] Martin, R; Howell, MD; Jaraquemada, D; Flerlage, M; Richert, J; Brostoff, S; Long, EO; McFarlin, DE; McFarland, HF. A myelin basic protein peptide is recognized by cytotoxic T cells in the context of four HLA-DR types associated with multiple sclerosis. *J. Exp. Med.* 1991, 173, 19-24.
- [69] Mantzourani, ED; Mavromoustakos, TM; Platts, JA; Matsoukas, JM; Tselios, T. Structural requirements for binding of myelin basic protein (MBP) peptides to MHC II: Effects on immune regulation. *Curr. Med. Chem.* 2005, 12, 1521-1535.
- [70] Rudolph, G; M.; Wilson, I. A. The specificity of TCR/pMHC interaction. *Curr. Opin. Immunol.* 2002, 14, 1043-1052.
- [71] Hare, BJ; Wyss, DF; Osburne, MS; Kern, PS; Reinherz, EL; Wagner, G. Structure, specificity and CDR mobility of a class II restricted single-chain T-cell receptor. *Nature Struct. Biol.* 1999, 6, 574-581.
- [72] Willcox, BE; Gao, GF; Wyer, JR; Ladbury, JE; Bell, JI; Jakobsen, BK; van der Merwe, PA. TCR binding to peptide-MHC stabilizes a flexible recognition interface. *Immunity* 1999, 10, 357-365.
- [73] Smith, KJ; Pyrdol, J; Gauthier, L; Wiley, DC; Wucherpennig, K. Crystal structure of HLA-DR2 (DRA*0101, DRB1*1501) complexed with a peptide from human myelin basic protein. *J. Exp. Med.* 1998, 188, 1511-1520.
- [74] Li, Y; Huang, Y.; Lue, J; Quandt, JA; Martin, R; Mariuzza, RA. Structure of a human autoimmune TCR bound to a myelin basic protein self-peptide and a multiple sclerosis-associated MHC class II molecule. *EMBO J.* 2005, 24, 2968-2979.
- [75] Tselios, T; Daliani, I; Deraos, S; Thymianou, S; Matsoukas, E; Troganis, A; Gerotheranassis, I; Mouzaki, A; Mavromoustakos, T; Probert, L; Matsoukas, J. Treatment of experimental allergic encephalomyelitis (EAE) by a rationally designed cyclic analogue of myelin basic protein (MBP) epitope 72-85. *Bioorg. Med. Chem. Lett.* 2000, 10, 2713-2717.
- [76] Matsoukas, J; Apostolopoulos, V; Kalbacher, H; Papini, AM; Tselios, T; Chatzantoni, K; Biagioli, T; Lolli, F; Deraos, S; Papathanassopoulos, P; Troganis, A; Mantzourani, E;

- [77] Mavromoustakos, T; Mouzaki, A. Design and synthesis of a novel potent myelin basic protein epitope 87-99 cyclic analogue: enhanced stability and biological properties of mimics render them a potentially new class of immunomodulators. *J. Med. Chem.* 2005, 48, 1470-1480.
- [78] Tselios, T; Apostolopoulos, V; Daliani, I; Deraos, S; Grdadolnik, S; Mavromoustakos, T; Melachrinou, M; Thymianou, S; Probert, L; Mouzaki, A; Matsoukas, J. Antagonistic effects of human cyclic MBP(87-99) altered peptide ligands in experimental allergic encephalomyelitis and human T-cell proliferation. *J. Med. Chem.* 2002, 45, 275-283.
- [79] Mantzourani, ED; Tselios, TV; Grdadolnik, SG; Platts, JA; Brancale, A; Deraos, G; Matsoukas, JM; Mavromoustakos, TM. Comparison of proposed putative active conformations of linear altered peptide ligands of myelin basic protein epitope 87-99 by spectroscopic and modelling studies: The role of position 91 and 96 in T-cell receptor activation. *J. Med. Chem.* 2006, 49, 6683-6691.
- [80] Mantzourani, ED; Tselios, TV; Grdadolnik, SG; Brancale, A; Platts, JA; Matsoukas, JM; Mavromoustakos, TM. A putative bioactive conformation for the altered peptide ligand of myelin basic protein and inhibitor of experimental autoimmune encephalomyelitis [Arg91, Ala96] MBP87-99 *J. Mol. Graphics Modell.* 2006, 25, 17-29.
- [81] Spyranti, A, Dalkas, G, Spyroulias, G, Mantzourani, E, Mavromoustakos, T, Firligou, I, Tselios, T. Putative bioactive conformations of amide linked cyclic myelin basic protein peptide analogues associated with experimental autoimmune encephalomyelitis. *J. Med. Chem* 2007, in press DOI: 10.1021/jm070770m.
- [82] Mantzourani, E.D., Blokar, K., Tselios, T.V., Matsoukas, J.M., Platts, J.A., Mavromoustakos, T.M., Grdadolnik S.G. A combined NMR and molecular dynamics simulation study to determine the conformational properties of agonists and antagonists against experimental autoimmune encephalomyelitis. *Bioorg. Med. Chem.* 2008, 16, 2171-2182.